Heliyon 9 (2023) e18008

Contents lists available at ScienceDirect

Heliyon

journal homepage: www.cell.com/heliyon

Transcriptome analysis identifies the role of Class I histone deacetylase in Alzheimer's disease

Fan Geng [a,1], Na Zhao [a,1], Xiu Chen [a], XueTing Liu [a], MengMeng Zhu [a], Ying Jiang [c], QingGuo Ren [a,b,*]

[a] School of Medicine, Southeast University, Nanjing, 210009, China
[b] Department of Neurology, Affiliated ZhongDa Hospital of Southeast University, Nanjing, 210009, China
[c] Department of Neurology, The 962nd Hospital of the PLA Joint Logistic Support Force, Harbin 150080, China

ARTICLE INFO

Keywords:
Class I HDACs
Alzheimer's disease
Diagnostic markers
WGCNA
HDAC1

ABSTRACT

Epigenetics modification is a process that does not change the sequence of deoxyribonucleic acid (DNA) in disease progression but can alter the genetic expression of the brain in Alzheimer's disease (AD). In this study, we deployed the weighted gene co-expression network analysis (WGCNA) to explore the role of Class I histone deacetylases (HDACs) in AD, which included HDAC1, HDAC2, HDAC3, and HDAC8. The aim of the study was to find how Class I HDACs affected AD pathology by analyzing the Gene Expression Omnibus (GEO) microarray datasets GSE33000. We found that HDAC1 and HDAC8 were more highly expressed in the cortex of AD patients than in Controls, while HDAC2 and HDAC3 were lower expressed. By WGCNA analysis, we found the blue module was associated with HDAC1 and HDAC8, and the turquoise module was related to HDAC2 and HDAC3. Functional enrichment analysis revealed that the Wnt signaling pathway and synaptic plasticity played an important role in the modification of HDAC1 and HDAC8 while gap junction and cell-cell junction were involved in the regulation of HDAC2 and HDAC3 in the disease progression of AD. By Receiver Operating Characteristics (ROC) analysis, we concluded that HDAC1 might be the most probable diagnostic biomarker of Class I HDACs for AD. Our study provided a comprehensive understanding of Class I HDACs and provided new insight into the function of HDAC1 in AD disease progression.

1. Introduction

Alzheimer's disease (AD) is a neurodegenerative disease characterized by progressive cognitive decline, memory loss, and behavioral deficits, which causes a huge burden to society. Amyloid-β (Aβ) and neurofibrillary tangles (NFTs) are the two main pathologies of AD. The results of epidemiological studies show that AD is the most common dementia and the percentage of dementia patients will double in Europe and triple worldwide by 2050 [1]. However, the mechanism of AD is still elusive and the current therapies are poorly effective. Thus, early detection of diagnostic biomarkers for AD will be of great significance for the treatment of AD. The identification of innovative diagnostic biomarkers and potential therapeutic targets is critical for developing

* Corresponding author. Department of Neurology, Affiliated ZhongDa Hospital, School of Medicine, Southeast University, Nanjing, Jiangsu, 210009, China.
E-mail address: renqingguo1976@163.com (Q. Ren).
[1] These authors contributed equally to this work.

https://doi.org/10.1016/j.heliyon.2023.e18008
Received 21 February 2023; Received in revised form 8 May 2023; Accepted 5 July 2023
Available online 6 July 2023
2405-8440/© 2023 The Authors. Published by Elsevier Ltd. This is an open access article under the CC BY-NC-ND license (http://creativecommons.org/licenses/by-nc-nd/4.0/).

disease-modifying therapies.

HDACs are one of the epigenetic modifications which participate in the progression of many neurodegenerative diseases, such as AD, Parkinson's disease (PD), Huntington's disease (HD) and so on [2,3]. Eighteen genes are included in the HDAC deacetylase family which is classified into four subtypes, Class I (HDAC1, 2, 3, 8), Class IIa (HDAC4, 5, 7, 9), Class IIb (HDAC6, 10), Class III (Sirtuin1-7) and Class IV (HDAC11) according to the different biological function and the locations in cells [4]. Research indicated that the Class I HDACs related pathway was activated in AD disease progression. It was evidenced that Class I HDACs family inhibitor BG45 can upregulate the expression of synapse-related proteins, repair cytoskeletal damage, and alleviate the apoptosis-mediated loss of hippocampal neurons in the early stage of AD cell model and animal model of APPswe/PS1dE9 (APP/PS1) mice [5–7]. Moreover, Martinostat Positron Emission Tomography (PET) analysis revealed that the expression of Class I HDACs (1–3) is reduced in AD patients and the decreased PET of Class I HDACs (1–3) in the AD brains was associated with the increased amyloid PET, tau PET concentration and cognitive decline [8]. All these results suggested that the Class I HDACs family may be a potential target for AD disease progression.

The previous study had identified the key role of Class I HDACs in AD pathology, but the expression of Class I HDACs varied greatly between studies and how Class I HDACs play an important role in AD remains unclear [6,9]. In this study, we aim to explore the relationship between Class I HDACs members including HDAC (1–3, 8) and AD patients cortex gene expression. GSE33000 was downloaded from Gene Expression Omnibus (GEO, https://www.ncbi.nlm.nih.gov/geo/) database and differential expression analyses were used to analyze the correlation with these factors. Pathway enrichment analysis by Gene Ontology (GO) and Kyoto Encyclopedia of Genes and Genomes (KEGG) and further analysis were integrated into our research. To date, no study has been conducted using WGCNA to explore the correlation between Class I HDACs and AD pathology. This study provided us with a better understanding of Class I HDACs biological function and a potential to find the potential biomarker in AD disease progression.

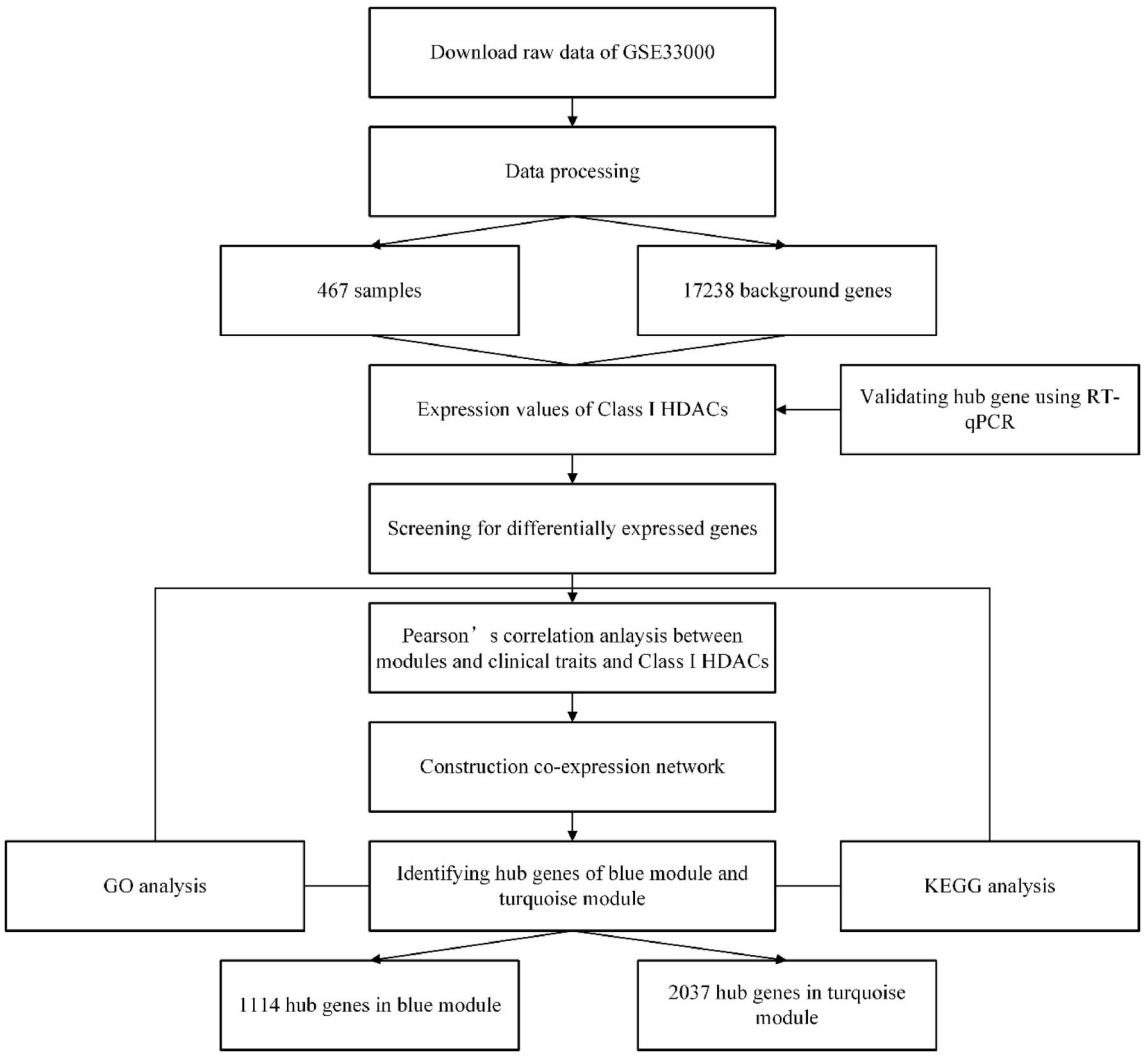

Fig. 1. Flow diagram of data preparation, processing, analysis, and validation.

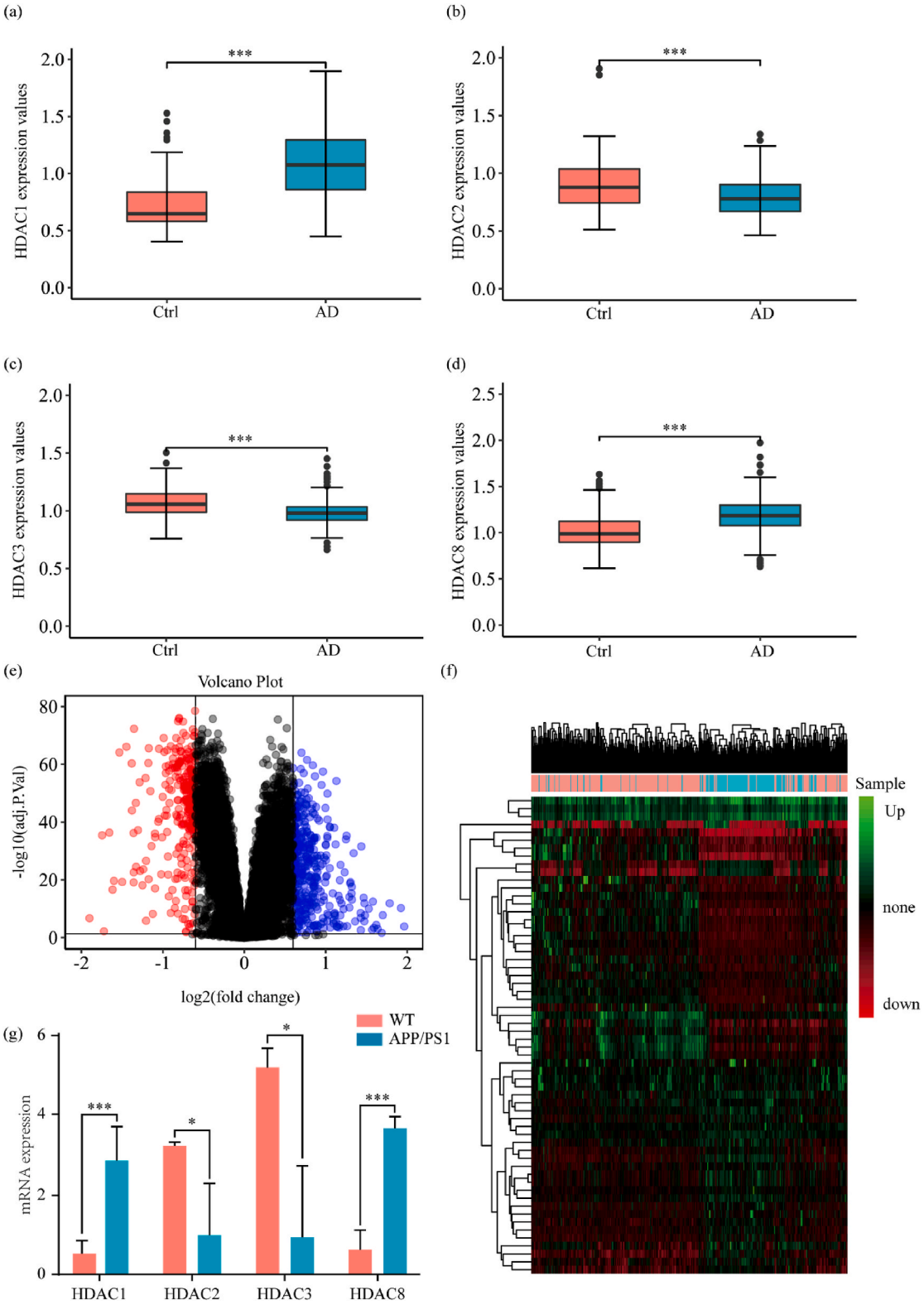

Fig. 2. Differential expression gene analysis. (a, b, c, d) HDAC1, HDAC2, HDAC3, HDAC8 expression between AD and non-demented controls. (HDAC1: [Con AD] ***P < 0.001, HDAC2: [Con AD] ***P < 0.001, HDAC3: [Con AD] ***P < 0.001, HDAC8: [Con AD] ***P < 0.001). (e) Blue, black, and red, indicate downregulated, non-significant, and upregulated DEGs, respectively. (f) The heatmap of the top 30 up- and down-regulated DEGs. (g) HDAC1, HDAC2, HDAC3, and HDAC8 mRNA expression between APP/PS1 mice and controls. (n = 3, 3 for group Con and AD

respectively. HDAC1: [Con AD] ***P < 0.001, HDAC2: [Con AD] *P = 0.0313, HDAC3: [Con AD] *P = 0.0124, HDAC8: [Con AD] ***P < 0.001) AD: Alzheimer's disease; Ctrl: non-demented controls; DEGs: differentially expressed genes. *P < 0.05, **P < 0.01, ***P < 0.001, *P versus Con group. (For interpretation of the references to color in this figure legend, the reader is referred to the Web version of this article.)

2. Materials and methods

2.1. Data source and microarray normalization

Gene expression profiles of human prefrontal cortex brain tissues GSE33000 were downloaded from the GEO database [10], including 157 non-demented controls and 310 AD patients. The samples of HD patients in this dataset were excluded from the study. This dataset was analyzed using Rosetta/Merck Human 44k 1.1 microarray platform (GPL4372). Microarray annotation information was downloaded from the GEO database to match probes with the genes. The datasets were normalized by log10 ratio [Cyanine(Cy) 5/Cy3] representing test/reference, we then used the *normalizeBetweenArray* function in the *limma* package to normalize the data [11]. All data were analyzed by R software (https://www.r-project.org/).

2.2. Identification of differentially expressed genes (DEGs)

DEGs were generated in the datasets using the *lmfit* and *eBayes* function of the *limma* package. The absolute value of log2 fold change $|\log FC| > 0.06$ and false discovery rate- (FDR-) adjusted $P < 0.05$ in the expression of individual genes were calculated to obtain the DEGs gene [12–14].

2.3. WGCNA network construction and module identification

The *WGCNA* package was used to construct a gene co-expression network and perform a module trait relationship to explore the most relevant modules and hub genes with Class I HDACs [15,16]. The gene co-expression network analysis was performed by clustering the DEGs with FDR adjusted $P < 0.05$. The *hclust* function was used to exclude the outliers from the samples. Firstly, the *pickSoftThreshold* function was used to determine the most appropriate power threshold. Secondly, the *adjacency* and *Topological overlap matrix (TOM) similarity* function was used to explore the similarity between these genes, and 1-TOM was used to calculate a pairwise distance to identify hierarchical clustering nodes and modules [17]. The minimum number of genes was set to 30 for the high reliability of the results. Thirdly, *hierarchical clustering* and the *dynamic tree cut* function were used to detect significant modules. Fourth, the gene significance (GS) and module membership (MM) were calculated to determine modules with clinical traits and HDAC1, HDAC2, HDAC3, and HDAC8. The corresponding gene information of significant modules was extracted according to geneModuleMembership > 0.8 and geneTraitSignificance > 0.2 for further analysis.

2.4. Functional enrichment analysis of significant module gene

The KEGG pathway enrichment analysis was performed by the *KEGG.db* package (https://bioconductor.org/) to identify functional attributes of the interested significant module genes and the most relevant twelve records were shown. A GO pathway enrichment analysis was conducted by the *clusterProfiler* package to identify the biological processes (BP), the molecular function (MF), and the cellular components (CC) in hub genes [18,19]. Significance was set to FDR adjusted $P < 0.05$. The most relevant five records were extracted and shown.

2.5. ROC curve analysis

The ROC analysis is a statistical method used to evaluate the performance of a binary classification model by plotting the true positive rate against the false positive rate at different classification thresholds. The ROC curve analysis was performed by the *pROC* package in R software to determine the area under the curve (AUC) for exploring the HDACs genes and evaluating their diagnostic value.

2.6. Quantitative polymerase chain reaction (qPCR)

Breeding of three ten months old APP/PS1 mice and its compared wt controls were purchased from Beijing Vital River Laboratory Animal Technology Co., Ltd. The genotype of the APP/PS1 mice was validated by PCR using DNA from the mice. After identification of the APP/PS1 genotype, the mice will be utilized for subsequent experiments. All procedures involving animals and their experiments were approved by the ethics committee of the Southeast University (No: 20220118050). The total RNA of the mice cortex was extracted by Trizol reagent (Invitrogen). The HiScript III RT SuperMix for qPCR Kit (Vazyme, Cat#Q711-02/03, Nanjing, China) was used to synthesize the cDNA with RNA, cDNA, primers (HDAC1: forward: TTCTGTCAGTTGTCCACGGG, reverse: TGAAGCAACCTAACCGGTCC; HDAC2: forward: GGAGGAGGCTACACAATCCG, reverse: TCTGGAGTGTTCTGGTTTGTCA; HDAC3: forward: GCCAAGACCGTGGCGTATT, reverse: GTCCAGCTCCATAGTGGAAGT; HDAC8: forward: CAGAGGAACCCGCCAACAG, reverse: CGCAGATGCTGACATACTCGG) and SYBR-Green PCR mix to perform the qPCR.

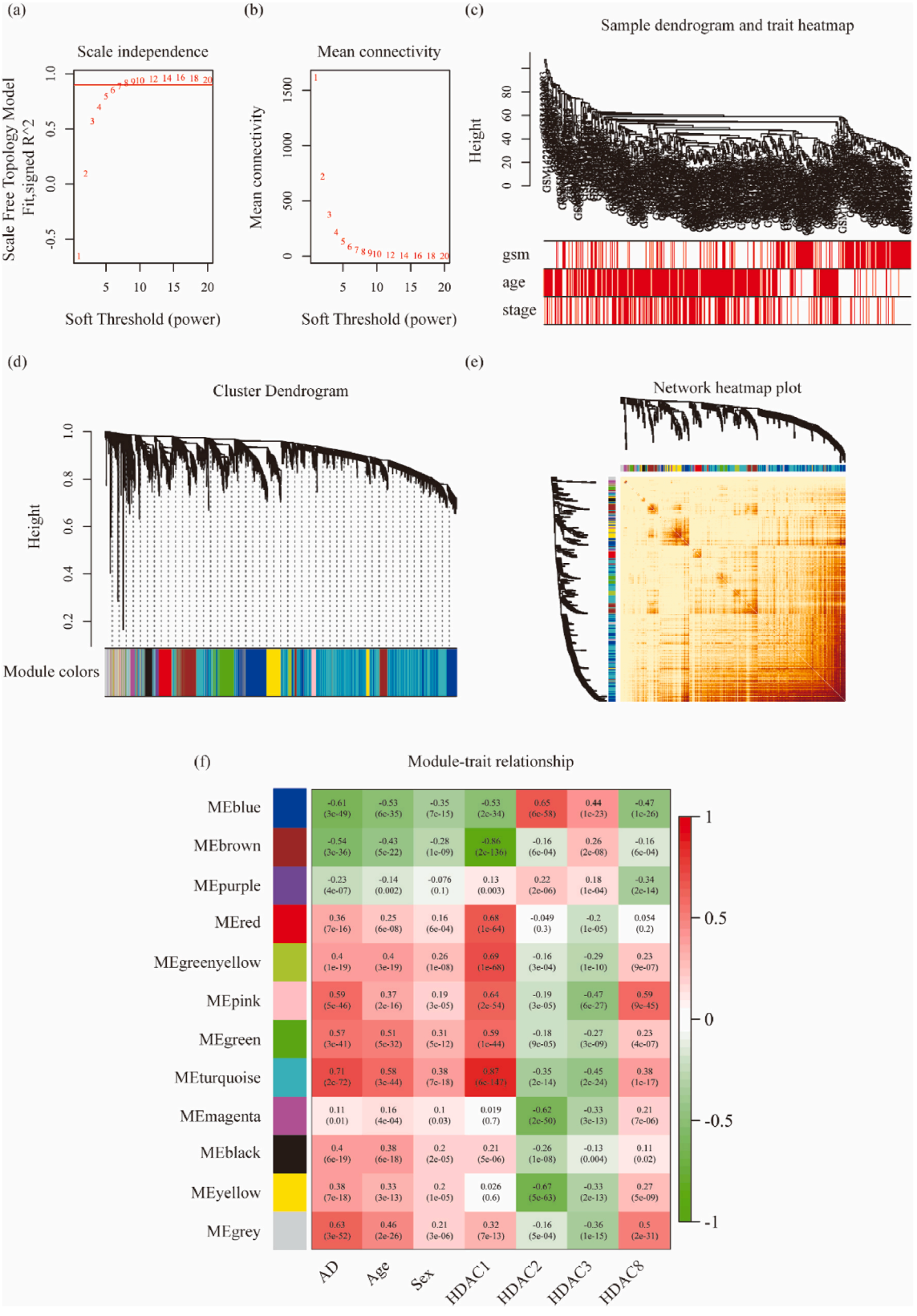

(caption on next page)

Fig. 3. Weighted correlation network analysis (WGCNA). (a, b) Determination of soft-threshold power for WGCNA. (c) Sample dendrogram and trait heatmap. (d) Twelve different colored modules are used to form a clustering dendrogram. (e) Heatmap plot depicting the co-expression topological overlap matrix (interaction patterns among genes using correlation as a measure of co-expression). (f) Grey stands for non-clustering genes, heatmap of module-trait relationship.

2.7. Statistical analysis

Data were expressed as mean values ± standard deviation (SD). Statistical significance was assessed using an unpaired Student's *t*-test. $P < 0.05$ was considered that there was significant difference between the groups.

3. Results

3.1. Identification of Class I HDACs expression and DEGs in the datasets

In this study, 157 non-demented controls and 310 AD patients were included for analysis. The flow diagram of this article was shown in Fig. 1. We first compared the expression values of HDAC1, HDAC2, HDAC3, and HDAC8 in the cortex of AD patients with non-demented controls in the datasets (Fig. 2a–d). The expression of HDAC1 and HDAC8 was higher in the AD group (1.08 ± 0.29 and 1.18 ± 0.19 respectively) compared to the Control (Ctrl) group (0.72 ± 0.22 and 1.03 ± 0.19 respectively) while the expression of HDAC2 and HDAC3 was lower in the AD group (0.80 ± 0.16 and 0.99 ± 0.11 respectively) compared to the Ctrl group (0.90 ± 0.22 and 1.08 ± 0.13 respectively). To verify the expression of HDACs in AD, we detected the expression in the cortical region of the brain of AD mice. In APP/PS1 mice cortex, the RNA expression values of HDAC1 and HDAC8 were higher when compared with the wt group while the HDAC2 and HDAC3 were lower expressed, which was in accordance with the gene expression values in dataset (Fig. 2g). After removing the unannotated and duplicated genes, 17,238 background genes were extracted for further differential genes analysis and total of 666 genes were determined as DEGs in AD patients compared with the non-demented group which selected by FDR adjust $P < 0.05$ and $|\log FC| > 0.6$. Among these genes, 377 DEGs were found to be upregulated significantly while 289 DEGs were downregulated (Fig. 2e). The cluster heatmap of DEGs of the top 30 upregulated and downregulated genes of DEGs were shown in Fig. 2f.

3.2. Gene Co-expression network construction of WGCNA

We used the standard that adj.P.Val < 0.05 to exclude the irrelevant genes. Then the top median expression of 5000 genes in 467 samples was included to construct the gene co-expression network of WGCNA at last. Firstly, we performed a sequence of 2–20 and used the *pickSoftThreshold* function to calculate the soft thresholding power β as 6 when the scale independence reached 0.9, to which the similarity of the genes was raised to calculate adjacency and TOMsimilarity (Fig. 3a and b). Next, we used the one step network construction function to split the samples into clusters, with a soft thresholding power set to 6, the deepSplit set to 2, and the minimum module size set to 30 (Fig. 3c).

Then we used *hierarchical clustering* and *dynamic tree cutting* functions to detect modules, in which the minimum size genes of the module were set to 30 (Fig. 3d). Finally, 12 gene modules were constructed. Then we performed a network heatmap plot (interconnectivity plot) of the gene network (Fig. 3e) together with the resulting modules and the corresponding hierarchical clustering dendrograms.

3.3. Construction of module trait relationship

The relationship between the co-expression gene modules and clinical sample traits, HDAC1, HDAC2, HDAC3 and HDAC8 were shown in Fig. 3f. As the heatmap showed, the turquoise module of 2037 genes had the strongest positive correlation with AD (correlation coefficient = 0.71, P = 2e-72) and HDAC1(correlation coefficient = 0.87, P = 6e-147). The blue module which had a total of 1114 genes had the most positive correlation with HDAC2(correlation coefficient = 0.65, P = 6e-58) and HDAC3(correlation coefficient = 0.44, P = 1e-23) while the most relevant positive module with HDAC3 was the pink module (correlation coefficient = 0.59, P = 9e-45), which had a total of 87 genes. Most positive modules related to HDAC1 and HDAC8 are the same, while most negative modules related to HDAC2 and HDAC3 are similar. Thus, we concluded that HDAC1 and HDAC8 had a similar effect and pathway in AD disease progression, and HDAC2 and HDAC3 had a similar effect on AD pathology.

3.4. Identification of Class I histon deacetylase related key modules

As shown in Fig. 4, we narrowed the 12 modules to the most two relevant modules with HDAC1, HDAC2, HDAC3 and HDAC8. The most two relevant modules with HDAC1 were turquoise and red (Fig. 4a and b), while the pink and turquoise modules were the most correlated with HDAC8 (Fig. 4g and h). In addition, the most significant module with HDAC2 and HDAC3 was the same and it's the blue module (Fig. 4c, e). The second relevant module with HDAC2 was the purple module while HDAC3 was the brown (Fig. 4d, f).

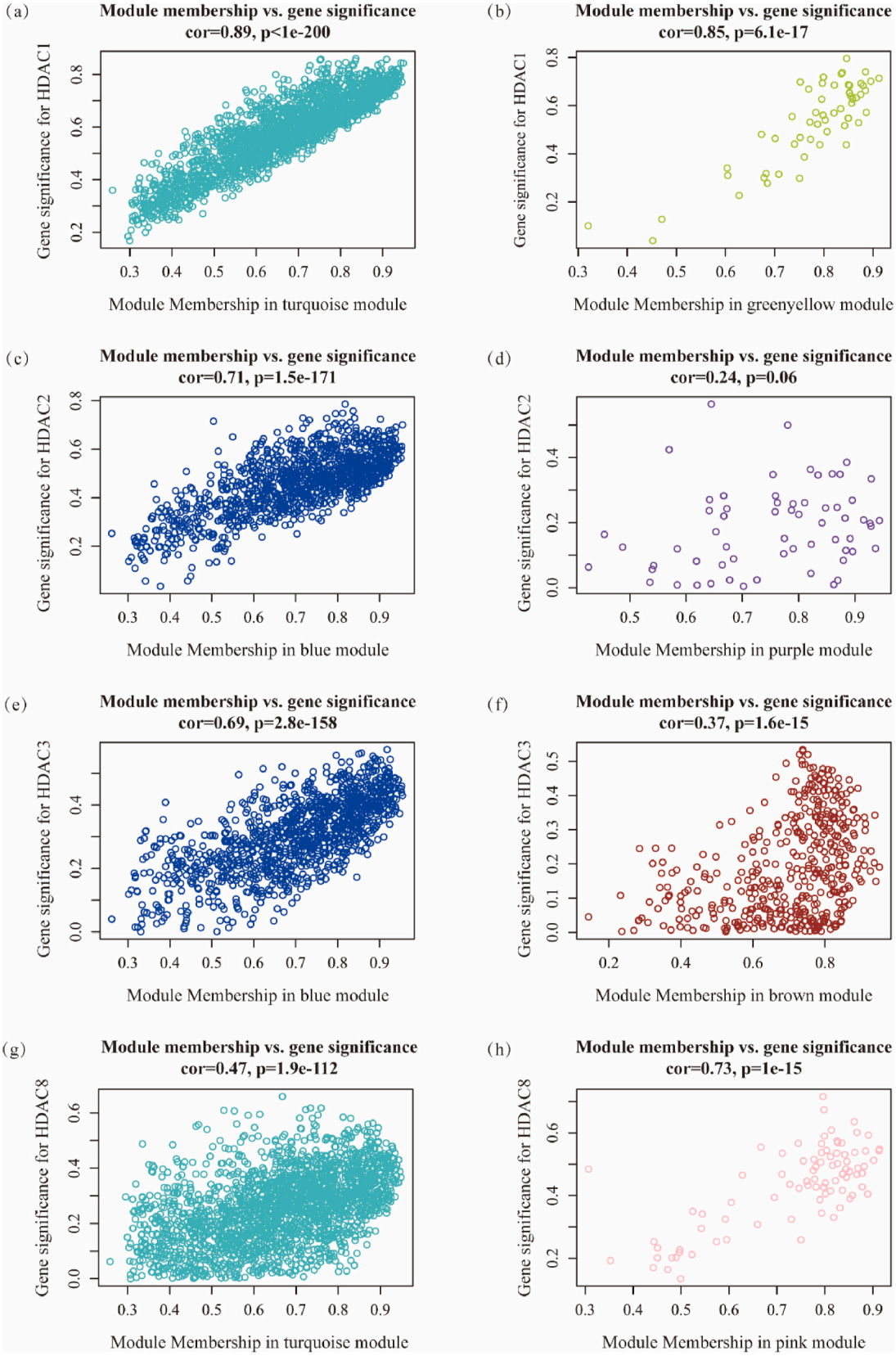

(caption on next page)

Fig. 4. Visualization of gene significance (GS) vs. module membership (MM). (a, b) Scatter represents the GS of HDAC1 and MM of the blue and green-yellow modules. (c, d) Scatter represents the GS of HDAC2 and MM of the blue and purple modules. (e, f) Scatter represents the GS of HDAC3 and MM of the blue and brown modules. (g, h) Scatter represents the GS of HDAC8 and MM of the turquoise and pink modules. (For interpretation of the references to color in this figure legend, the reader is referred to the Web version of this article.)

3.5. Functional enrichment analysis

Then we performed a KEGG analysis and GO enrichment analysis on blue and turquoise module hub genes because the red, purple, brown, and pink modules had too less genes to analyze. As shown in Fig. 5a, the top 15 hub genes in the blue module were exported to cytoscape to construct an interactional map. It was indicated that Hypoxanthine Phosphoribosyltransferase 1 (HPRT1), Serpin Family I Member 1 (SERPINI1), p21 (RAC1) Activated Kinase 3 (PAK3), Voltage Dependent Anion Channel 2 (VDAC2), Neural EGFL Like 2 (NELL2), Voltage Dependent Anion Channel 1 (VDAC1), and so on are central genes in the blue module. In addition, significant genes in turquoise were mapped to Cytoscape in Fig. 5b. *N*-ethylmaleimide Sensitive Factor, Vesicle Fusing ATPase (NSF), Protocadherin Alpha 4 (PCDHA4), Secretogranin V (SCG5), MLLT11 Transcription Factor 7 Cofactor (MLLT11), Regulator of G Protein Signaling 7 (RGS7), Protocadherin Alpha 12 (PCDHA12), and so on were the significant genes in the turquoise module. By KEGG analysis, we found that the Wnt signaling pathway, Long-term potential, Neurotrophin signaling pathway and so on had a significant correlation with HDAC1 and HDAC8 in the progression of AD (Fig. 5c). Furthermore, we discovered that synapse organization, learning or memory, synaptic membrane and glutamatergic synapse pathway participated in the blue module by GO enrichment analysis (Fig. 5e). In addition, the most relevant pathway with HDAC2 and HDAC3 were gap junction and Extracellular Matrix (ECM) -receptor interaction by KEGG analysis (Fig. 5d). Additionally, by GO enrichment analysis, except cell-cell junction and extracellular matrix structural constituent, HDAC2 and HDAC3 participated in the renal system development, epithelial cell proliferation, kidney development, and so on (Fig. 5f).

3.6. Verifying the diagnostic value of Class I histone deacetylase

We performed the ROC curve line with HDAC1, HDAC2, HDAC3 and HDAC8 expression values(Fig. 6a–d). The ROC curves were given to estimate their specificity and sensitivity. The area under the curve (AUC) of HDAC1, HDAC2, HDAC3 and HDAC8 were 0.839, 0.649, 0.720 and 0.741 between AD patients VS. non-demented control, indicating that HDAC1 might be a prospective biomarker and diagnostic value for AD.

4. Discussion

It was reported that five HDAC inhibitors had already been approved by Food and Drug Administration (FDA) for the clinical treatment of cancer [20,21]. Previous studies had reported that HDAC1 modulated OGG-1-initiated 8-oxoguanine (8-oxoG) repair in the brain and activation of HDAC1 alleviated the deleterious effects of 8-oxoG in AD mouse models compared with the wt control [22]. Furthermore, it is indicated that HDAC3 interacted with tau and inhibition of HDAC3 improved recognition and spatial memory in the AD mouse model [23]. In addition, Exifone, a drug which activated the deacetylase activity of Class I HDACs, was effective in improving cognitive decline associated with AD and PD [24]. However, the expression of Class I HDACs in AD varied greatly between studies. And how the Class I HDACs are involved in AD remains unclear.

In our study, we used a novel transcriptome data analysis method to analyze the roles of HDACs in Alzheimer's disease. We built a gene co-expression network to analyze the correlations between Class I HDACs with AD-related genes. After WGCNA analysis, we identified the blue module was significantly correlated with HDAC1 and HDAC8 and the turquoise module was much more related with HDAC2 and HDAC3. We conducted the pathway enrichment function that HDAC1 and HDAC8 had a similar function to regulate the long-term potential, synaptic plasticity, Wnt signaling pathway and tau binding of AD disease progression while HDAC2 and HDAC3 have a similar pathway on the ECM receptor interaction, cell-cell junction, gap junction and other diseases, such as renal system development, urogenital system development, kidney development and so on. Thus, we concluded that HDAC1 and HDAC8 are more related to AD pathology while HDAC2 and HDAC3 have a wider impact on many other diseases.

Synapses are specific junctions for communication between neurons, or between neurons and muscle cells or glands [25,26]. Synaptic dysregulation is one of the main causes of memory loss in AD [27]. The intensity of synaptic transmission relies on changes in neuron activity, where the long-term depression (LTD) and long-term potential (LTP) act as the fundamental mechanism of learning and memory [28]. Ganesh et al. showed that treated the mice with human brain soluble Aβ protein oligomers reduced the dendritic spine density, inhibited the LTP and enhanced the LTD in normal rodent mice hippocampus [29]. In this study, we found that HDAC1 and HDAC8 participated in the modification of long-term potential, synapse organization, learning and memory, regulation of neuron projection development, and synaptic membrane. Furthermore, the analysis indicated that the hub genes in the blue module were associated with tau protein binding. It provided us with new insight into the regulation function of HDAC1 and HDAC8 in AD disease progression.

Wingless-type MMTV integration site family (Wnt) signaling pathway is an essential growth pathway which participated in the progression of cell proliferation and programmed cell death [30]. It is indicated that Wnt co-receptor Low-Density Lipoprotein Receptor-Related Protein 6 (LRP6) dysfunction led to the loss of functional and structural integrity of synapse interaction connections in the adult brain [31]. Additionally, increasing expression of Wnt signaling inhibitors Dickkopf-1 (Dkk1) caused a synapse

(caption on next page)

Fig. 5. Visualization of hub genes. (a, b) The top 20 hub genes in the blue and turquoise modules. (c, d) Gene Ontology (GO) analysis of hub genes in the blue and turquoise modules. (e, f) Kyoto Encyclopedia of Genes and Genomes (KEGG) analysis of hub genes in the blue and turquoise modules. (For interpretation of the references to color in this figure legend, the reader is referred to the Web version of this article.)

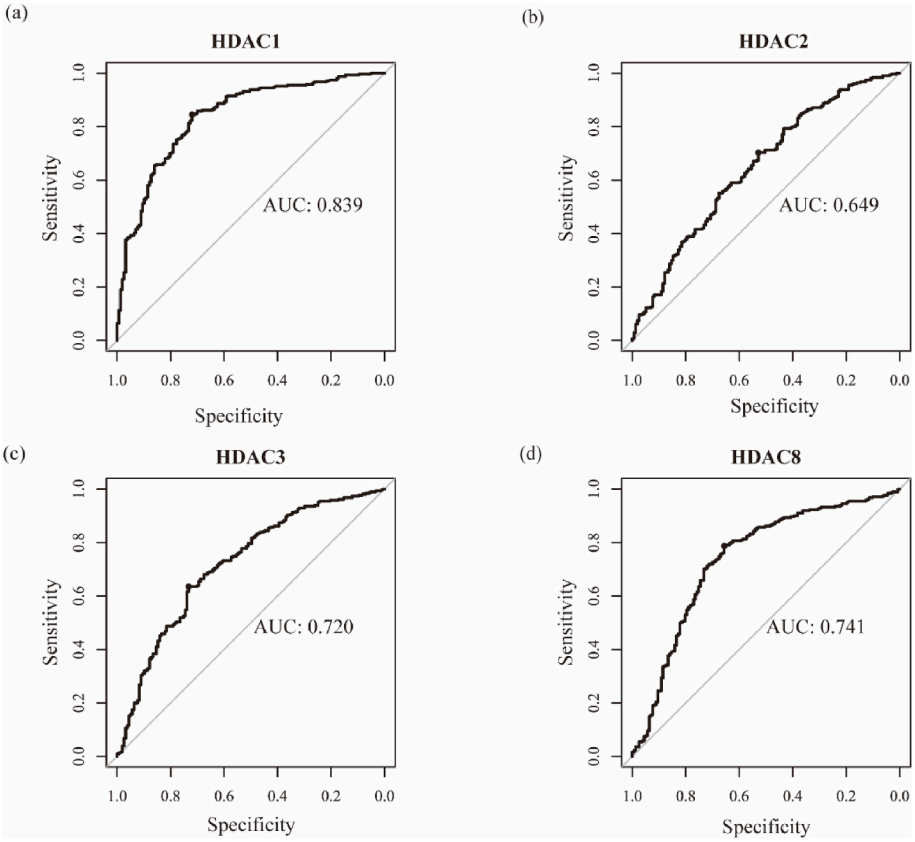

Fig. 6. Visualization of AUC line. (a, b, c, d) Performance evaluation of AUC analysis of HDAC1, HDAC2, HDAC3, and HDAC8.

dysfunction raised by amyloid deposition. Numerous evidences had indicated that increased HDAC1 expression activated the Wnt pathway [32,33]. This is in line with our results that HDAC1 and HDAC8 participated in the Wnt pathway activation. Mitogen-Activated Protein Kinase (MAPK) is a kinase has a key role in the insulin pathway which affects gene expression and memory formation [34]. Absence of insulin, not insulin resistance led to the dysfunction of the insulin signaling pathway resulted in the formation of toxic $A\beta_{1\text{-}42}$ and phosphated tau (p-tau) oligomers [35]. In this study, we found that the MAPK pathway and neurotrophin signaling pathway were involved in the biological regulation of HDAC1 and HDAC8 with AD. All these pathways played a prominent role in AD pathology [36–40]. Our study provided a new therapy discovery on the impact of HDAC1 and HDAC8 involved in the neuropathology and genesis of AD and provided a supportive proof how HDAC8 participated in AD disease progression.

Mitochondria is an organelle that played key roles in neuron differentiation and adult neuroplasticity development. Mitochondria dysfunction was the cause of Aβ deposition and tau phosphorylation which led to cognitive abnormalities [41,42]. Voltage-dependent anion channel (VDAC) which was located in the outer membrane of mitochondria. Research showed that the VDAC can bind to Aβ, leading the mitochondria dysfunction in the progression of AD [43,44]. In our study, we identified that mitochondria-associated proteins VDAC1 and ATP2A2 engaged in the regulation of HDAC1 and HDAC8 of the AD brain. In the hub genes of turquoise, we found that PCHDA5, PCDHA12, and PCDHAC2 were involved in the HDAC2 and HDAC3 regulation. They were the PCDHA family, members of the protocadherin alpha gene cluster, which played a critical role in the establishment and function of specific cell-cell connections in the brain. Cell-cell connection dysfunction was involved in many diseases, such as renal system development, kidney development and urogenital system development [45–47]. It indicated that HDAC2 and HDAC3 are a broad spectrum of disease targets. In summary, our results demonstrated that HDAC1 and HDAC8 were more relevant with AD pathology while HDAC2 and HDAC3 are more correlated with many other diseases and they are a broad spectrum of disease targets. According to the AUC results, HDAC1 may be the most therapeutic diagnosis value and biomarker of the four Class I HDACs in the progression of AD pathology.

In conclusion, the current study aimed to use an integrated bioinformatic approach to identify the effective therapeutic targets and find the potential biomarker in the four Class I HDACs in the genesis and molecule progression of AD. Our results suggested a set of

pathways that HDAC1, HDAC2, HDAC3, and HDAC8 participated for further investigation into the modification of DNA and molecular mechanism of AD. Nevertheless, further molecular experimental verification is needed to confirm the function of Class I HDACs in the disease progression of AD. Proteomic analysis or integrated bioinformatic approach is needed to further determine the regulatory role of HDACs in AD disease.

Author contribution statement

Qingguo Ren: Conceived and designed the experiments; Analyzed and interpreted the data; Contributed reagents, materials, analysis tools or data.

Fan Geng, Na Zhao, Xiu Chen: Wrote the paper; Performed the experiments; Analyzed and interpreted the data.

Xueting Liu, Mengmeng Zhu, Ying Jiang: Analyzed and interpreted the data; Contributed reagents, materials, analysis tools or data.

Data availability

The data that support the findings of this study are openly available in GEO datasets of NCBI at [https://www.ncbi.nlm.nih.gov/geo/query/acc.cgi?acc=GSE33000], reference number [10].

Declaration of competing interest

The authors declare that they have no known competing financial interests or personal relationships that could have appeared to influence the work reported in this paper

Acknowledgments

This research was supported by the National Natural Science Foundation of China (81870850).

References

[1] P. Scheltens, et al., Alzheimer's disease, Lancet 397 (10284) (2021) 1577–1590.
[2] F. He, et al., Design, synthesis and biological evaluation of dual-function inhibitors targeting NMDAR and HDAC for Alzheimer's disease, Bioorg. Chem. 103 (2020), 104109.
[3] N. Macabuag, et al., Developing HDAC4-selective protein degraders to investigate the role of HDAC4 in Huntington's disease pathology, J. Med. Chem. 65 (18) (2022) 12445–12459.
[4] V. Kumar, et al., Understanding the role of histone deacetylase and their inhibitors in neurodegenerative disorders: current targets and future perspective, Curr. Neuropharmacol. 20 (1) (2022) 158–178.
[5] Y. Han, et al., A Class I HDAC inhibitor Rescues synaptic damage and neuron loss in APP-transfected cells and APP/PS1 mice through the GRIP1/AMPA pathway, Molecules 27 (13) (2022) 4160.
[6] T.A. Pascoal, et al., [11C]Martinostat PET analysis reveals reduced HDAC I availability in Alzheimer's disease, Nat. Commun. 13 (1) (2022) 4171.
[7] Y. Han, et al., Class I HDAC inhibitor improves synaptic proteins and repairs cytoskeleton through regulating synapse-related genes in vitro and in vivo, Front. Aging Neurosci. 12 (2020), 619866.
[8] T.A. Pascoal, et al., [(11)C]Martinostat PET analysis reveals reduced HDAC I availability in Alzheimer's disease, Nat. Commun. 13 (1) (2022) 4171.
[9] J.S. Guan, et al., HDAC2 negatively regulates memory formation and synaptic plasticity, Nature 459 (7243) (2009) 55–60.
[10] M. Narayanan, et al., Common dysregulation network in the human prefrontal cortex underlies two neurodegenerative diseases, Mol. Syst. Biol. 10 (7) (2014) 743.
[11] M.E. Ritchie, et al., Limma powers differential expression analyses for RNA-sequencing and microarray studies, Nucleic Acids Res. 43 (7) (2015) e47.
[12] J.D. Storey, A direct approach to false discovery rates, J. Roy. Stat. Soc. B (Stat. Methodol.) 64 (3) (2002) 479–498.
[13] J.D. Storey, R. Tibshirani, Statistical significance for genomewide studies, Proc. Natl. Acad. Sci. U. S. A. 100 (16) (2003) 9440–9445.
[14] J.D. Storey, J.E. Taylor, D.O. Siegmund, Strong control, conservative point estimation and simultaneous conservative consistency of false discovery rates: a unified approach, J. Roy. Stat. Soc. B (Stat. Methodol.) (2004) 66.
[15] B. Zhang, S. Horvath, A general framework for weighted gene co-expression network analysis, Stat. Appl. Genet. Mol. Biol. 4 (2005) Article17.
[16] P. Langfelder, S. Horvath, WGCNA: an R package for weighted correlation network analysis, BMC Bioinf. 9 (2008) 559.
[17] P. Langfelder, et al., Is my network module preserved and reproducible? PLoS Comput. Biol. 7 (1) (2011), e1001057.
[18] T. Wu, et al., clusterProfiler 4.0: a universal enrichment tool for interpreting omics data, Innovation (Camb). 2 (3) (2021), 100141.
[19] G. Yu, et al., clusterProfiler: an R package for comparing biological themes among gene clusters, OMICS 16 (5) (2012) 284–287.
[20] Y. Li, et al., Zinc-dependent deacetylase (HDAC) inhibitors with different zinc binding groups, Curr. Top. Med. Chem. 19 (3) (2019) 223–241.
[21] Y. Li, et al., Zinc-dependent deacetylases (HDACs) as potential targets for treating Alzheimer's disease, Bioorg. Med. Chem. Lett 76 (2022), 129015.
[22] P.-C. Pao, et al., HDAC1 modulates OGG1-initiated oxidative DNA damage repair in the aging brain and Alzheimer's disease, Nat. Commun. 11 (1) (2020) 2484.
[23] K.J. Janczura, et al., Inhibition of HDAC3 reverses Alzheimer's disease-related pathologies in vitro and in the 3xTg-AD mouse model, Proc. Natl. Acad. Sci. U. S. A. 115 (47) (2018), E11148-E11157.
[24] D. Patnaik, et al., Exifone is a potent HDAC1 activator with neuroprotective activity in human neuronal models of neurodegeneration, ACS Chem. Neurosci. 12 (2) (2021) 271–284.
[25] D.J. Selkoe, Alzheimer's disease is a synaptic failure, Science 298 (5594) (2002) 789–791.
[26] J.E. Hamos, L.J. DeGennaro, D.A. Drachman, Synaptic loss in Alzheimer's disease and other dementias, Neurology 39 (3) (1989) 355.
[27] Z. Chen, et al., Epigenetic regulation of synaptic disorder in Alzheimer's disease, Front. Neurosci. 16 (2022), 888014.
[28] E. Tönnies, E. Trushina, Oxidative stress, synaptic dysfunction, and Alzheimer's disease, J Alzheimers Dis. 57 (4) (2017) 1105–1121.
[29] G.M. Shankar, et al., Amyloid-beta protein dimers isolated directly from Alzheimer's brains impair synaptic plasticity and memory, Nat. Med. 14 (8) (2008) 837–842.
[30] R. Nusse, H. Clevers, Wnt/β-Catenin signaling, disease, and emerging therapeutic modalities, Cell 169 (6) (2017) 985–999.
[31] J. Buechler, P.C. Salinas, Deficient Wnt signaling and synaptic vulnerability in Alzheimer's disease: emerging roles for the LRP6 receptor, Front. Synaptic Neurosci. 10 (2018) 38.

[32] Y. Zeng, et al., HDAC1 regulates inflammation and osteogenic differentiation of ankylosing spondylitis fibroblasts through the Wnt-Smad signaling pathway, J. Orthop. Surg. Res. 17 (1) (2022) 343.
[33] Z. Liu, et al., WNT signaling promotes Nkx2.5 expression and early cardiomyogenesis via downregulation of Hdac1, Biochim. Biophys. Acta 1793 (2) (2009) 300–311.
[34] A. Sędzikowska, L. Szablewski, Insulin and insulin resistance in Alzheimer's disease, Int. J. Mol. Sci. 22 (18) (2021) 9987.
[35] T. Imamura, et al., Insulin deficiency promotes formation of toxic amyloid-β42 conformer co-aggregating with hyper-phosphorylated tau oligomer in an Alzheimer's disease model, Neurobiol. Dis. 137 (2020), 104739.
[36] J.K. Lee, N.J. Kim, Recent advances in the inhibition of p38 MAPK as a potential strategy for the treatment of Alzheimer's disease, Molecules 22 (8) (2017) 1287.
[37] C. Falcicchia, et al., Involvement of p38 MAPK in synaptic function and dysfunction, Int. J. Mol. Sci. 21 (16) (2020) 5624.
[38] J. Tulloch, et al., Maintained memory and long-term potentiation in a mouse model of Alzheimer's disease with both amyloid pathology and human tau, Eur. J. Neurosci. 53 (2) (2021) 637–648.
[39] A. Doulah, G. Mahmoodi, M. Pourmahdi Borujeni, Evaluation of the pre-treatment effect of Centella asiatica medicinal plants on long-term potentiation (LTP) in rat model of Alzheimer's disease, Neurosci. Lett. 729 (2020), 135026.
[40] M. Amidfar, et al., The role of CREB and BDNF in neurobiology and treatment of Alzheimer's disease, Life Sci. 257 (2020), 118020.
[41] J.S. Kerr, et al., Mitophagy and Alzheimer's disease: cellular and molecular mechanisms, Trends Neurosci. 40 (3) (2017) 151–166.
[42] I.W. Weidling, R.H. Swerdlow, Mitochondria in Alzheimer's disease and their potential role in Alzheimer's proteostasis, Exp. Neurol. 330 (2020), 113321.
[43] M. Manczak, P.H. Reddy, Abnormal interaction of VDAC1 with amyloid beta and phosphorylated tau causes mitochondrial dysfunction in Alzheimer's disease, Hum. Mol. Genet. 21 (23) (2012) 5131–5146.
[44] A. Atlante, et al., Dysfunction of mitochondria in Alzheimer's disease: ANT and VDAC interact with toxic proteins and aid to determine the fate of brain cells, Int. J. Mol. Sci. 23 (14) (2022) 7722.
[45] S. Rayego-Mateos, et al., Interplay between extracellular matrix components and cellular and molecular mechanisms in kidney fibrosis, Clin. Sci. (Lond.) 135 (16) (2021) 1999–2029.
[46] G. Coticchio, et al., Oocyte maturation: gamete-somatic cells interactions, meiotic resumption, cytoskeletal dynamics and cytoplasmic reorganization, Hum. Reprod. Update 21 (4) (2015) 427–454.
[47] A. Abed, et al., Connexins in renal endothelial function and dysfunction, Cardiovasc. Hematol. Disord.: Drug Targets 14 (1) (2014) 15–21.